PHYSICAL REVIEW D **86,** 036013 (2012)

Extended Simpson's rule for the screened Cornell potential in momentum space

Jiao-Kai Chen*

School of Physics and Information Science, Shanxi Normal University, Linfen 041004, China

(Received 29 November 2011; published 29 August 2012)

We employ the Nyström method with the extended Simpson's rule to solve numerically the Schrödinger equation in momentum space with the screened Cornell potential. Two peculiar phenomena, furcation and deviation of the first point, occur in the obtained eigenfunctions. By applying the Landé subtraction method to remove or relieve the singularities in the integrands, the furcation phenomenon disappears, the deviation of the first point is weakened, and the obtained eigenvalues have high accuracy.

DOI: 10.1103/PhysRevD.86.036013 PACS numbers: 11.10.St, 02.60.Nm, 03.65.Ge, 12.39.Pn

I. INTRODUCTION

The Cornell potential model (or the funnel potential model), incorporating a linear term at large distances and a color-coulomb term at short distances [1–5], has been successful in describing the spectra for both charmonia and bottomonia. However, this kind of model will overestimate the masses of heavy quarkonia above the open-flavor thresholds, such as $\Upsilon(6S)$ and $\chi'_{c2}/Z(3930)$ [6], and will not be reliable in the domain beyond the open-charm threshold probably because of the screening of the linear potential due to light $q\bar{q}$ pairs' creation out of the vacuum between the two heavy-quark sources. In recent years, the screened potential models have been applied to calculate the heavy quarkonium spectrum, spin-spin splittings, radiative decays, and leptonic decay widths [7–10], as well as the spectra of light hadrons [11,12].

During the last few decades, analytic and numerical studies [13–27] have been performed. In this paper, we employ the Landé subtraction method [28–37] to remove the momentum-space singularities [38] in the screened Cornell potential. We implement the Nyström method with the extended Simpson's rule to solve numerically the Schrödinger equation with the screened Cornell potential which incorporates the screened color-Coulomb potential and the screened linear potential. The obtained results appear good, but some peculiar phenomena emerge when we try to make the parameters become small. In the numerical results, we observe two unexpected peculiar phenomena. One is named as furcation, to distinguish it from bifurcation in nonlinear problem, that the obtained eigenfunctions divide into two branches. More details can be found in Ref. [39]. Another is the deviation of the first point in the eigenfunctions which is smaller than expected. Applying the Landé subtraction method, and then solving numerically the subtracted Schrödinger equation using the same method, the furcation phenomenon disappears and the deviation is weakened.

In Sec. II, we deal analytically with the Schrödinger equation with the screened Cornell potential in momentum space and then treat it numerically in Sec. III. In Sec. IV, the numerical results are given. The conclusions are in Sec. V.

II. ANALYTICAL TREATMENT OF THE SCHRÖDINGER EQUATION IN MOMENTUM SPACE

By letting $\hbar = c = 1$, the Schrödinger equation reads in coordinate space

$$E\psi(\mathbf{r}) = -\frac{1}{2\mu}\nabla^2\psi(\mathbf{r}) + V(\mathbf{r})\psi(\mathbf{r}). \tag{1}$$

By taking the Fourier transform

$$\begin{aligned}\phi(\mathbf{p}) &= \int \psi(\mathbf{r})e^{-i\mathbf{p}\cdot\mathbf{r}}d\mathbf{r},\\ \psi(\mathbf{r}) &= (2\pi)^{-3}\int \phi(\mathbf{p})e^{i\mathbf{p}\cdot\mathbf{r}}d\mathbf{p},\end{aligned} \tag{2}$$

the Schrödinger Eq. (1) in momentum space takes the form

$$E\phi(\mathbf{p}) = \frac{p^2}{2\mu}\phi(\mathbf{p}) + \frac{1}{(2\pi)^3}\int V(\mathbf{q})\phi(\mathbf{p}')d\mathbf{p}', \tag{3}$$

where $\mathbf{q} \equiv \mathbf{p} - \mathbf{p}'$.

The well-known Cornell potential (or the funnel potential)

$$V = -\frac{\alpha}{r} + \lambda r, \tag{4}$$

contains the perturbative expectation plus an additional linear term. In this paper, the screened Cornell potential is considered

$$\begin{aligned}V_{\mathrm{SC}} = V_c + V_Y + V_L, \qquad V_c = C, \qquad V_Y = -\frac{\alpha}{r}e^{-\beta r},\\ V_L = \frac{\lambda}{\eta}(1 - e^{-\eta r}),\end{aligned} \tag{5}$$

where V_c is the constant potential, V_Y is the screened Coulomb potential (or the Yukawa potential) which approaches the Coulomb potential when $\beta \to 0$, V_L is the screened confinement potential which becomes linear potential as $\eta \to 0$, $\lim_{\eta\to 0} V_L = \lambda r$. β is the screening

*chenjk@sxnu.edu.cn

parameter of the screened Coulomb potential. η is the screening factor for the screened linear potential which makes the long-range scalar part of $V_L(r)$ flat when $r \gg 1/\eta$ and still linearly rising when $r \ll 1/\eta$, λ is the string tension, and $\alpha = (4\alpha_s)/3$, α_s being the strong coupling constant of the color Coulomb potential. Sometimes, the screening parameters β and η are introduced mathematically to avoid the divergence in potential in numerical calculations, or to regularize the infrared divergence. $V_{\rm SC}$ approaches the Cornell potential as $\beta,\ \eta \to 0$.

By the Fourier transform

$$V(\mathbf{q}) = \int V'(\mathbf{r}) e^{-i\mathbf{q}\cdot\mathbf{r}} d\mathbf{r}, \qquad V'(\mathbf{r}) = (2\pi)^{-3} \int V(\mathbf{q}) e^{i\mathbf{q}\cdot\mathbf{r}} d\mathbf{q}, \tag{6}$$

the potentials in (5) read in momentum space

$$V_{\rm SC} = V_c + V_Y + V_L, \qquad V_c(\mathbf{q}) = (2\pi)^3 C\delta(\mathbf{q}), \qquad V_Y(\mathbf{q}) = -\frac{4\pi\alpha}{\beta^2 + q^2}, \qquad V_L(\mathbf{q}) = (2\pi)^3 \frac{\lambda}{\eta}\left\{\delta(\mathbf{q}) + \frac{1}{2\pi^2}\frac{\partial}{\partial\eta}\left[\frac{1}{\eta^2 + q^2}\right]\right\}. \tag{7}$$

During the derivation of the preceding equations, we have used the definition of the delta function

$$\delta(\mathbf{q}) = (2\pi)^{-3} \int e^{-i\mathbf{q}\cdot\mathbf{r}} d\mathbf{r}, \qquad \delta(\mathbf{r}) = (2\pi)^{-3} \int e^{i\mathbf{q}\cdot\mathbf{r}} d\mathbf{q}. \tag{8}$$

Then using the expansion formula

$$\frac{1}{x - t} = \sum_{l=0}^{\infty} (2l + 1) Q_n(x) P_n(t), \tag{9}$$

where $Q_n(z)$ is the Legendre polynomial of the second kind, the orthogonality of the Legendre polynomials

$$\int_{-1}^{1} P_m(x) P_n(x) dx = \frac{2}{2n + 1}\delta_{mn}, \tag{10}$$

the addition of spherical harmonics

$$P_l(\cos\Theta) = \frac{4\pi}{2l + 1} \sum_{m=-l}^{l} Y_{lm}(\Omega) Y^*_{lm}(\Omega'), \tag{11}$$

the orthogonality of spherical harmonics

$$\int d\Omega Y^*_{lm}(\Omega) Y_{l'm'}(\Omega) = \delta_{l'l}\delta_{m'm}, \tag{12}$$

the delta function represented in the spherical coordinates

$$\delta(\mathbf{p} - \mathbf{p}') = \frac{\delta(p - p')\delta(\theta - \theta')\delta(\phi - \phi')}{p^2 sin\theta}, \tag{13}$$

and

$$V^l(p, p') = \int d\Omega Y^*_{lm}(\Omega) \int d\Omega' Y_{l'm'}(\Omega') V(\mathbf{q}), \tag{14}$$

the potentials (7) expanded in partial waves are written as

$$\begin{aligned} V^l_{\rm SC}(p, p') &= V^l_c(p, p') + V^l_Y(p, p') + V^l_L(p, p'), \\ V^l_c(p, p') &= (2\pi)^3 C \frac{\delta(p - p')}{p^2}\delta_{ll'}, \\ V^l_Y(p, p') &= -8\pi^2\alpha \frac{Q_l(z')}{pp'}, \\ V^l_L(p, p') &= (2\pi)^3 \left[\frac{\lambda}{\eta}\frac{\delta(p - p')}{p^2}\delta_{ll'} + \frac{\lambda}{\pi}\frac{Q'_l(z)}{(pp')^2}\right], \end{aligned} \tag{15}$$

where $z' = (p^2 + p'^2 + \beta^2)/(2p'p)$, $z = (p^2 + p'^2 + \eta^2)/(2p'p)$. $Q'_l(z)$ is the first derivative of $Q_l(z)$ with respect to z.

Expanding the momentum space wave function $\phi(\mathbf{p})$ in partial waves,

$$\phi(\mathbf{p}) = \sum_{nlm} a_{nlm}\phi_{nl}(p) Y_{lm}(\Omega), \tag{16}$$

where a_{nlm}'s are coefficients of the expansion, and then integrating over the solid angle, the Schrödinger equation in momentum space (3) is rewritten in partial wave form as

$$E_{nl}\phi_{nl}(p) = \frac{p^2}{2\mu}\phi_{nl}(p) + \frac{1}{(2\pi)^3}\int p'^2 dp' V^l_{\rm SC}(p, p')\phi_{nl}(p'). \tag{17}$$

From Eq. (15) and the relations

$$Q_l(z) = P_l(z)Q_0(z) - w_{l-1}(z), \qquad Q_0(z) = \frac{1}{2}\ln\frac{z + 1}{z - 1}, \qquad w_{l-1}(z) = \sum_{m=1}^{l}\frac{1}{m}P_{l-m}(z)P_{m-1}(z), \tag{18}$$

it is obvious that the singularities of $V^l_Y(p, p')$ and $V^l_L(p, p')$ come from the singularities of $Q_0(z')$, $Q_0(z)$ and $Q'_0(z)$. $Q_0(z)$ has logarithmic singularity as $z \to 1$, and $Q'_0(z)$ exhibits a second order pole at $p = p'$ as $\eta \to 0$. As shown in Ref. [39], the numerical results obtained by solving numerically the integral Eq. (17) are still bad even though there is no singularity in the integrands when the factors β and η are small. Therefore, the Landé subtraction method is necessary not only for the

Coulomb potential but also for the screened Coulomb potential, and for the screened Cornell potential.

There are two useful identities

$$\int_0^\Lambda \frac{1}{p'} Q_0(z)dp' = \frac{1}{2}\Big[Li_2\Big(-\frac{i\Lambda}{\eta - ip}\Big) - Li_2\Big(\frac{i\Lambda}{\eta - ip}\Big) + Li_2\Big(\frac{i\Lambda}{\eta + ip}\Big) - Li_2\Big(-\frac{i\Lambda}{\eta + ip}\Big)\Big],$$
$$\int_0^\Lambda Q_0'(z)dp' = -\frac{p}{\eta}\Big[(p + i\eta)\arctan\frac{\Lambda}{\eta - ip} + (p - i\eta)\arctan\frac{\Lambda}{\eta + ip}\Big], \quad (19)$$

where $Li_2(z)$ is the Spence's function (or the dilogarithm), a particular case of the polylogarithm. As Λ approaches infinity, the above equations become [34–37]

$$\int_0^\infty \frac{1}{p'} Q_0(z)dp' = \frac{\pi^2}{2} - \pi\arctan\frac{\eta}{p},$$
$$\int_0^\infty Q_0'(z)dp' = -\frac{\pi p^2}{\eta}. \quad (20)$$

Employing the identities (20) to subtract out the singularities, and then using the identity $P_l'(1) = l(l+1)/2$, the momentum space Schrödinger equation with the screened Cornell potential (17) is written as

$$E_{nl}\phi_{nl}(p) = \Big[\frac{p^2}{2\mu} + C\Big]\phi_{nl}(p) - \Big[\frac{\pi^2}{2} - \pi\arctan\frac{\beta}{p}\Big]\frac{\alpha}{\pi}p\phi_{nl}(p) + \Big[\frac{\pi^2}{2} - \pi\arctan\frac{\eta}{p}\Big]\frac{\lambda}{\pi p}\frac{l(l+1)}{2}\phi_{nl}(p)$$
$$- \frac{\alpha}{\pi p}\int_0^\infty P_l(z')\frac{Q_0(z')}{p'}\Big[p'^2\phi_{nl}(p') - \frac{p^2\phi_{nl}(p)}{P_l(z')}\Big]dp' + \frac{\lambda}{\pi p^2}\int_0^\infty P_l(z)Q_0'(z)\Big[\phi_{nl}(p') - \frac{\phi_{nl}(p)}{P_l(z)}\Big]dp'$$
$$+ \frac{\lambda}{\pi p^2}\int_0^\infty P_l'(z)\frac{Q_0(z)}{p'}\Big[p'\phi_{nl}(p') - \frac{l(l+1)}{2}\frac{p\phi_{nl}(p)}{P_l'(z)}\Big]dp' + \frac{1}{\pi p^2}\int_0^\infty [\alpha p p' w_{l-1}(z') - \lambda w_{l-1}'(z)]\phi_{nl}(p')dp'. \quad (21)$$

The δ term in the linear potential V_L^l cancels out the integral of Q_0^l in Eq. (20). This equation is free of singularities if $\eta > 0$. When $p = p'$, the integrands of the first integral and of the third integral are zero whether $\beta = 0$ and $\eta = 0$ or not, while the integrand of the second integral is left with a principal-value singularity if $\eta = 0$, and is singularity-free if $\eta > 0$. The Eq. (21) is free of logarithmic singularity and the sever singularity from double-pole is weakened by subtraction to be a principal-value singularity.

III. NUMERICAL TREATMENT OF THE SCHRÖDINGER EQUATION IN MOMENTUM SPACE

A. Nodes of wave functions

From the Eq. (2), we can obtain

$$\phi_{nl}(p) = (-1)^l 4\pi i^l \int j_l(pr)\psi_{nl}(r)r^2 dr, \quad (22)$$

where $j_l(pr)$ gives the spherical Bessel function of the first kind. In the calculation of the preceding equation, the following formulas are used

$$e^{ikr\cos\Theta} = 4\pi\sum_{m=0}^{\infty}\sum_{n=-m}^{m} i^m j_m(kr)Y_{mn}^*(\Omega')Y_{mn}(\Omega), \quad (23)$$

and

$$P_m(-x) = (-1)^m P_m(x). \quad (24)$$

It is known that the nodes of the wave functions $\psi_{nl}(r)$ in coordinate space for the Schrödinger equation with the Coulomb potential or with the linear potential distribute over the whole range $(0, \infty)$, and the nodes of the corresponding wave functions in momentum space $\phi_{nl}(p)$ [the counterparts of $\psi_{nl}(r)$] congregate on the finite range $(0, M)$, M is a finite number. Based on the transform formula (22), we provide a simple, intuitive explanation. The spherical Bessel function $j_l(pr)$ is an oscillating and decreasing function, and the wave function $\psi_{nl}(r)$ is a decreasing function, too. A node of the wave function $\phi_{nl}(p)$ demands that the negative part of the product of the function $j_l(pr)$ and the wave function $\psi_{nl}(r)$ cancels out the positive part of the product at the node point p. As p is large, the function $j_l(pr)$ will oscillate violently and decrease quickly. Therefore, it makes the wave function $\phi_{nl}(p)$ more difficult to be zero. While if p is small, it will be easier for the wave function $\phi_{nl}(p)$ to be zero. The fact is the nodes of the wave function $\phi_{nl}(p)$ lie in a finite interval. Similarly, it is expected that the nodes of the wave function in momentum space will congregate over the finite interval for the screened Cornell potential problem. This is one base on which the truncation method can be applied.

Because the wave function in momentum space decreases quickly and the nodes of it lie in the finite range, we can truncate the range at a large finite value Λ. If Λ is large enough and the step length for a given quadrature rule is small enough, we can expect to obtain the numerical results with enough accuracy. On the contrary, we cannot

get high accurate numerical results for the same problem in the coordinate space only by diminishing step size because some nodes of the wave function $\psi_{nl}(r)$, especially for the highly excited states, go outside the finite interval.

B. Truncation method

For the convenience of discussing the truncation method, the partial wave Schrödinger equation in momentum space (17) is written in the form

$$E\phi(p) = \int_0^\infty K(p, p')\phi(p')p'^2 dp', \tag{25}$$

$$K(p, p') = \frac{1}{2\mu}\delta(p - p') + \frac{1}{(2\pi)^3}V^\ell(p, p'). \tag{26}$$

It can be rewritten as

$$E\phi(p) = E'\phi(p) + R_\epsilon + R_\Lambda(p), \tag{27}$$

where

$$\begin{aligned} E'\phi(p) &= \int_\epsilon^\Lambda K(p, p')\phi(p')p'^2 dp', \\ R_\epsilon(p) &= \int_0^\epsilon K(p, p')\phi(p')p'^2 dp', \\ R_\Lambda(p) &= \int_\Lambda^\infty K(p, p')\phi(p')p'^2 dp'. \end{aligned} \tag{28}$$

Obviously, the following equation [26,40]

$$\tilde{E}\tilde{\phi}(p) = \int_\epsilon^\Lambda K(p, p')\tilde{\phi}(p')p'^2 dp', \quad p, p' \in (\epsilon, \Lambda), \tag{29}$$

is also an eigenvalue integral equation. When $\epsilon \to 0$ and $\Lambda \to \infty$, we can have $\tilde{E} \to E$ and $\tilde{\phi}(p) \to \phi(p)$. If $R_\Lambda(p)$ and $R_\epsilon(p)$ is small enough, the Eq. (29) will be a good approximation to Eq. (25).

From Eqs. (27) and (28), we have

$$\eta(\epsilon, \Lambda) = \frac{E - E'}{E} = \frac{(\int_0^\epsilon + \int_\Lambda^\infty)K(p, p')\phi(p')p'^2 dp'}{\int_0^\infty K(p, p')\phi(p')p'^2 dp'}. \tag{30}$$

There is an expansion theorem [41] for the eigenvalue integral Eq. (25)

$$K(p, p') = \sum_{i=1}^\infty E_i\phi_i(p)\phi_i^\dagger(p'), \tag{31}$$

where $\phi_i(p)$ is the ith normalized wave function, E_i is the ith eigenvalue. Substituting the formula (31) into Eq. (30), we obtain

$$\eta_j(\epsilon, \Lambda) = \frac{E_j - E'_j}{E_j} = \varepsilon_{\epsilon j} + \varepsilon_{\Lambda j}, \tag{32}$$

where

$$\begin{aligned} \varepsilon_{\epsilon j} &= \int_0^\epsilon \phi_j^\dagger(p')\phi_j(p')p'^2 dp', \\ \varepsilon_{\Lambda j} &= \int_\Lambda^\infty \phi_j^\dagger(p')\phi_j(p')p'^2 dp'. \end{aligned} \tag{33}$$

$\eta_j(\epsilon, \Lambda)$ decreases with the decrease of ϵ and with the increase of Λ.

Dividing Eq. (29) by Eq. (27), we have

$$\begin{aligned} &\left[1 + \frac{\tilde{E} - E}{E}\right]\left[1 + \frac{\tilde{\phi} - \phi}{\phi}\right] \\ &\quad = \left[1 + \frac{\int_\epsilon^\Lambda K(p, p')(\tilde{\phi} - \phi)p'^2 dp'}{\int_\epsilon^\Lambda K(p, p')\phi p'^2 dp'}\right] \\ &\qquad \times \left[1 + \frac{(\int_0^\epsilon + \int_\Lambda^\infty)K(p, p')\phi p'^2 dp'}{\int_\epsilon^\Lambda K(p, p')\phi p'^2 dp'}\right]^{-1}. \end{aligned} \tag{34}$$

Therefore, it is obtained for small $\eta(\epsilon, \Lambda)$

$$\frac{E - \tilde{E}}{E} \approx \frac{(\int_0^\epsilon + \int_\Lambda^\infty)K(p, p')\phi(p')p'^2 dp'}{\int_\epsilon^\Lambda K(p, p')\phi(p')p'^2 dp'} = \frac{\eta(\epsilon, \Lambda)}{1 - \eta(\epsilon, \Lambda)}. \tag{35}$$

From Eqs. (32) and (35), it is obvious that $\tilde{E} > E$ if $E < 0$, and $\tilde{E} < E$ if $E > 0$. The Eq. (35) gives the relative error estimate of $\tilde{E}$ for the truncation method.

In Table I, we give the rough estimates of the orders of ε_ϵ and ε_Λ for the ground state wave function $\phi_{10}(p)$ of the hydrogen atom with the Coulomb potential. The variation of the orders of ε_ϵ and ε_Λ with the principal number n are listed in Table II.

C. Nyström method

The bound state suggests its wave functions will decrease quickly, therefore the truncated method can behave well, which are consistent with the Eqs. (33) and (35). Then we apply the Nyström method with the extended

TABLE I. Estimates of the orders of ε_ϵ and ε_Λ for the ground state $\phi_{10}(p)$ of the hydrogen atom. (In the atomic units.)

$\epsilon =$	10^{-1}	10^{-2}	10^{-3}	10^{-5}
$\varepsilon_\epsilon \sim$	10^{-3}	10^{-6}	10^{-9}	10^{-15}
$\Lambda =$	10	50	100	200
$\varepsilon_\Lambda \sim$	10^{-5}	10^{-9}	10^{-10}	10^{-12}

TABLE II. Variation of the orders of ε_ϵ and ε_Λ with the principal number n. $l = 0$, $\epsilon = 10^{-5}$, $\Lambda = 20$. (In the atomic units.)

$n =$	1	3	5	10
$\varepsilon_\epsilon \sim$	10^{-15}	10^{-12}	10^{-11}	10^{-10}
$\varepsilon_\Lambda \sim$	10^{-6}	10^{-8}	10^{-8}	10^{-9}

Simpson's rule to solve the truncated integral Eq. (29). It is well-known that the extended Simpson rule reads

$$\int_{x_1}^{x_N} f(x)dx = h\Big[\frac{1}{3}f_1 + \frac{4}{3}f_2 + \frac{2}{3}f_3 + \frac{4}{3}f_4 + \cdots + \frac{2}{3}f_{N-2} + \frac{4}{3}f_{N-1} + \frac{1}{3}f_N\Big] + O(h^4). \tag{36}$$

Adopting the extended Simpson's rule to approximate the integrals, the truncated form of the integral Eq. (17) becomes the matrix equation

$$E\phi_i = T_i\phi_i + \sum_{j=1}^{N} V_{ij}\phi_j w_j. \tag{37}$$

For convenience, $\tilde{E}$ is written as E, $\tilde{\phi}$ is written as ϕ in the above equation and in the following discussions. In Eq. (37), $T_i = p_i^2/(2\mu)$, ϕ_j is shorthand notation for $\phi_{nl}(p_j)$, N is the number of points; $p_1 = \epsilon$, $p_N = \Lambda$; p_i and w_i are the abscissas and the corresponding weights for a given quadrature rule; and V_{ij} is defined as

$$V_{ij} = \Big[C + \frac{\lambda}{\eta}\Big]\delta_{ij} - \frac{\alpha}{\pi}\frac{p_j'}{p_i}Q_l(z_{ij}') + \frac{\lambda}{\pi p_i^2}Q_l'(z_{ij}). \tag{38}$$

For the screened potential, the factors β and η can be small but finite, there will be no singularities in V_{ij} at point $p = p'$. When the screening parameters β and η are large, the obtained numerical results are good, while when they become small, the numerical results are unexpected. The obtained eigenfunctions divide into two branches as p is small. The two branches approach each other as p increases and converge at one point into one line, see Fig. 1. And the first points of the obtained eigenfunctions are smaller than expected. These two peculiar phenomena arise from the bad behaviors of the potentials, i.e., the integrals cannot be well approximated by the extended Simpson's rule when β and η are small. Therefore, the subtraction method is needed to remove the singularities at $p = p'$.

Employing the truncation method and the extended Simpson's rule, the less singular integral Eq. (21) can be approximated by the matrix equation

$$E\phi_i = T_i\phi_i + V_{ii}\phi_i + \sum_{j\neq i}^{N} V_{ij}\phi_j w_j, \tag{39}$$

where $T_i = p_i^2/(2\mu)$. The potential term V_{ij} is defined as

$$V_{ij} = -\frac{\alpha}{\pi}\frac{p_j'}{p_i}P_l(z_{ij}')Q_0(z_{ij}') + \frac{\lambda}{\pi p_i^2}P_l(z_{ij})Q_0'(z_{ij}) + \frac{1}{\pi p_i^2}[\alpha p_i p_j' w_{l-1}(z_{ij}') - \lambda w_{l-1}'(z_{ij})] + \frac{\lambda}{\pi p_i^2}P_l'(z_{ij})Q_0(z_{ij}) \quad \text{if i} \neq \text{j}, \tag{40}$$

and

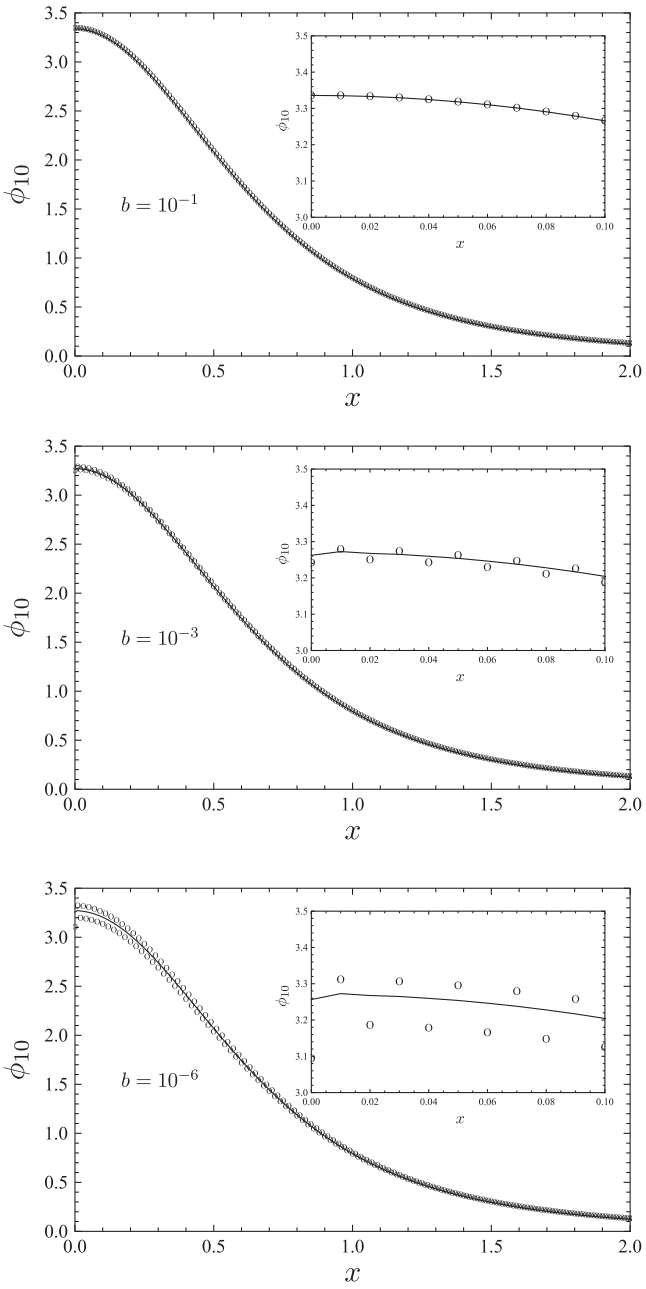

FIG. 1. The comparison between the ground state eigenfunctions for the subtracted equation (the solid line) (39) and for the original equation (the circles) (37) with the screened Coulomb potential. The extended Simpson's rule is applied to solve numerically the eigenvalue equations. $b = \beta/(\mu\alpha)$, $x = p/(\mu\alpha)$, $\lambda = 0$.

$$V_{ii} = C\delta_{ii} + \frac{\lambda}{\eta}\delta_{ii} - \frac{\alpha}{\pi}p_i A_i(\beta) + \frac{\lambda l(l+1)}{2p_i}A_i(\eta) + \frac{\lambda}{\pi p_i^2}B_i + \sum_{j\neq i}^{N}\Big[\frac{\alpha}{\pi}\frac{p_i}{p_j'}Q_0(z_{ij}') - \frac{\lambda l(l+1)}{2\pi}\frac{Q_0(z_{ij})}{p_i p_j'} - \frac{\lambda}{\pi p_i^2}Q_0'(z_{ij})\Big]w_j, \tag{41}$$

where

$$A_i(\beta) = \frac{1}{2}\Big[Li_2\Big(-\frac{i\Lambda}{\beta - ip_i}\Big) - Li_2\Big(\frac{i\Lambda}{\beta - ip_i}\Big) + Li_2\Big(\frac{i\Lambda}{\beta + ip_i}\Big) - Li_2\Big(-\frac{i\Lambda}{\beta + ip_i}\Big)\Big],$$

$$B_i = -\frac{p_i}{\eta}\Big[(p_i + i\eta)\arctan\frac{\Lambda}{\eta - ip_i} + (p_i - i\eta)\arctan\frac{\Lambda}{\eta + ip_i}\Big].$$

In Eq. (41), the formula (19) for a finite interval $(0, \Lambda)$ is used instead of the formula (20) for an infinite interval $(0, \infty)$.

D. Effects of parameters on eigenvalues

In coordinate space, the Hamiltonian for a central potential problem is given by

$$H = T - \frac{\alpha}{r}e^{-\beta r} + \frac{\lambda}{\eta}(1 - e^{-\eta r}), \tag{42}$$

where

$$T = -\frac{1}{2\mu}\frac{d^2}{dr^2} + \frac{l(l+1)}{2\mu r^2}.$$

Applying the Hellmann-Feynman theorem, we have

$$\begin{aligned}
\frac{\partial E_n}{\partial \alpha} &= \left\langle nlm \left| \frac{\partial H}{\partial \alpha} \right| nlm \right\rangle < 0,\\
\frac{\partial E_n}{\partial \beta} &= \left\langle nlm \left| \frac{\partial H}{\partial \beta} \right| nlm \right\rangle > 0,\\
\frac{\partial E_n}{\partial \lambda} &= \left\langle nlm \left| \frac{\partial H}{\partial \lambda} \right| nlm \right\rangle > 0,\\
\frac{\partial E_n}{\partial \eta} &= \left\langle nlm \left| \frac{\partial H}{\partial \eta} \right| nlm \right\rangle < 0.
\end{aligned} \tag{43}$$

From the preceding relations, it is obvious that the eigenvalues will increase with the increases of β and λ, and with the decreases of α and η. The numerical results are in agreement with this conclusion.

When β is very small, the wave function for the screened Coulomb potential will approximate the wave function for the Coulomb potential whose analytical form is well known. Then using the second formula in Eq. (43), we have the eigenvalues for the ground state and for the first radial excited state for the screened Coulomb potential

$$\begin{aligned}
E_1 &= -\frac{\mu\alpha^2}{2} + \Big[\mu\alpha - \frac{4\mu^3\alpha^3}{(\beta + 2\mu\alpha)^2}\Big],\\
E_2 &= -\frac{\mu\alpha^2}{8} + \Big[\frac{\mu\alpha}{4} - \frac{\mu^3\alpha^3(2\beta^2 + \mu^2\alpha^2)}{4(\beta + \mu\alpha)^4}\Big].
\end{aligned} \tag{44}$$

The similar formula for higher excited states can be obtained in the same way. Constructing a power series expansion for the above two formula to order β^2, we have

$$E_1 \approx -\frac{\mu\alpha^2}{2} + \beta - \frac{3\beta^2}{4\mu\alpha},$$

$$E_2 \approx -\frac{\mu\alpha^2}{8} + \beta - \frac{3\beta^2}{\mu\alpha}.$$

IV. NUMERICAL RESULTS

As noted in the preceding section, the wave function in momentum space decreases quickly and the nodes of the wave functions lie in a finite range. Therefore, we rewrite the singular integral Eq. (17) and the subtracted integral Eq. (21) in the form of Eq. (29), respectively, by truncating the infinite range at a lower limit ϵ and an upper limit Λ, then transform the truncated integral equations into the matrix Eqs. (37) and (39) by employing the Nyström method with the Simpson's rule. Equations (37) and (39) are standard algebraic eigenvalue problems and can be solved easily. In this paper, the Schrödinger equations with the screened Coulomb potential, the screened linear potential, and the screened Cornell potential are numerically solved. Two peculiar phenomena, furcation and deviation of the first point, are observed in the obtained eigenfunctions.

A. Screened Coulomb potential

1. Eigenfunctions

Applying the truncation method and the Nyström method with the extended Simpson's rule, solving numerically the integral Eq. (17), i.e., solving the matrix Eq. (37), the numerical results are obtained. When β is large, the results are good and reliable; when β becomes small, two peculiar phenomena emerge. One is furcation [39] that the eigenfunctions divide into two branches at small x and converge into one as x increases. The points of the furcated solution lie above and under the subtracted equation solution alternatively and form two forks, that is to say, the furcated solution oscillates around the subtracted equation solution. The furcated wave function is one solution and not two solutions close to each other; hence there is not artificial degeneracy. Another is the deviation of the first point of the eigenfunctions, i.e., the first point is smaller than expected.

As displayed in Fig. 1, there occur the furcation phenomenon and the deviation of the first point as b (or β), which is small when the extended Simpson's rule is adopted. The furcation and the deviation of the first point are weakened as b increases and will disappear if b is large enough. The peculiar phenomenon arise from both the singularities of the integrands and the extended Simpson's rule. When b is small, the integrands have stronger singularities and the integrals cannot be well approximated by the extended Simpson's rule, and the furcation occurs; when b is large, the integrands are less singular so that the integrals can be well approximated by the extended Simpson's rule, and the peculiar phenomena disappear.

If the extended trapezoidal rule instead of the extended Simpson's rule is applied to solve the matrix Eq. (37), there is not furcation phenomenon in the obtained eigenfunctions, see Fig. 2. Different weights for the extended Simpson's rule and for the extended trapezoidal rule make them different. We find the unequal repeated weights and the bad behavior of the integrands give rise to the furcation phenomenon. Therefore, the furcation phenomenon is an indicator whether the integrals can be well approximated by the extended Simpson's rule, so, in this sense, the extended Simpson's rule gets an advantage over the extended trapezoidal rule.

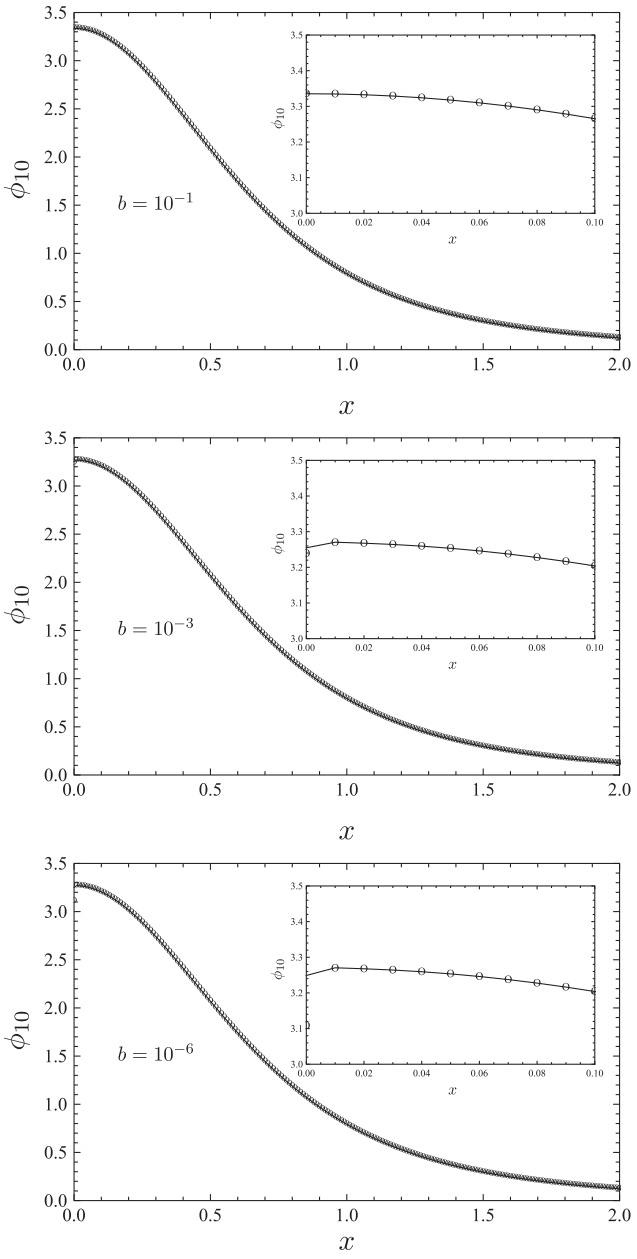

FIG. 2. The comparison between the ground state eigenfunctions for the subtracted equation (the solid line) (39) and for the original equation (the circles) (37) with the screened Coulomb potential. The extended trapezoidal rule is applied to solve numerically the eigenvalue equations. $b = \beta/(\mu\alpha)$, $x = p/(\mu\alpha)$, $\lambda = 0$.

The deviations of the first points in the obtained eigenfunctions emerge in both the extended Simpson's rule and the extend trapezoidal rule, see Figs. 1 and 2. It arise also from the singularities of the integrands. The smaller is b, the more singular are the integrands; therefore, the integrands will behave worse and cannot be well approximated; as a result, the peculiar phenomena occur.

We adopt the Landé subtraction method to remove the logarithmic singularity and then solve the subtracted integral Eq. (21), i.e., solve the matrix Eq. (39). The obtained eigenfunctions are free of furcation, and the deviation is alleviated. As shown in Figs. 1 and 2, the solid lines representing the results for the subtracted integral equation have no branches, and the deviation of the first point is relieved.

The furcation phenomenon and the deviation phenomenon not only emerge in the eigenfunction for the ground state but also in the eigenfunctions for the excited states. The subtraction method works for them all.

2. Eigenvalues

The eigenvalues obtained by the extended Simpson's rule and by the extended trapezoidal rule are listed in Table III. As b (or β) is large, the eigenvalues of the matrix Eq. (37) agree well with the eigenvalues of the matrix Eq. (39), so the subtraction method is not necessary. As b decreases, the error will be large because of the bad behaviors of the integrands, the subtraction method is required.

The eigenvalues with different screening parameter b and different truncation parameter x_N (or Λ) are listed in Table IV. It is obvious that the eigenvalues converge quickly to reach the stable results for increasing x_N. Clearly, the obtained results are calculated with very high accuracy and so reliable. The Landé subtraction method employed in the calculations can be easily extended to other cases.

B. Screened linear potential

Employing the Nyström method with the extended Simpson's rule, the furcation in the obtained eigenfunctions for the screened linear potential are stronger than for the screened Coulomb potential, see Fig. 3. This is because the linear potential has a double-pole singularity, while the Coulomb potential is logarithmically singular. Similarly, the furcation phenomenon disappears when the subtraction method is applied. There is no deviation phenomenon in the eigenfunctions for the screened linear potential due to the delta function in the linear potential. We also note another interesting result that the left principal-value singularity does not induce the furcation phenomenon when the extended Simpson's rule is employed.

TABLE III. The ratios $E_n/(\mu\alpha^2)$ for the screened Coulomb potential with $l = 0$. $b = \beta/(\mu\alpha)$, $x = p/(\mu\alpha)$, $\lambda = 0$. $x_1 = 10^{-6}$, $x_N = 5$, $h = 0.01$. TR denotes the extended trapezoidal rule, and SR represents the extended Simpson's rule; C represents the subtracted Eq. (39), and NC the original Eq. (37).

b	n	TR(C)	TR(NC)	SR(C)	SR(NC)
	1	−0.397455	−0.397331	−0.397414	−0.397331
10^{-1}	2	−0.0489009	−0.0488742	−0.0488922	−0.0488742
	3	−0.00307495	−0.00306958	−0.00307324	−0.00306958
	1	−0.489253	−0.491555	−0.489212	−0.492217
10^{-3}	2	−0.122762	−0.125155	−0.122752	−0.125835
	3	−0.0542015	−0.0566106	−0.054201	−0.0573194
	1	−0.490251	−0.513594	−0.49021	−0.51679
10^{-6}	2	−0.123758	−0.147192	−0.123748	−0.150749
	3	−0.0551941	−0.0786442	−0.0551937	−0.0827475

TABLE IV. The ratios $E_n/(\mu\alpha^2)$ for the screened Coulomb potential with $l = 0$. $b = \beta/(\mu\alpha)$, $x = p/(\mu\alpha)$, $\lambda = 0$. $x_1 = 10^{-6}$, $h = 0.01$. The subtracted Eq. (39) is solved by using the extended Simpson's rule.

x_N	n	$b = 0$	$b = 10^{-6}$	$b = 10^{-3}$	$b = 10^{-1}$
	1	−0.490211	−0.49021	−0.489212	−0.397414
5	2	−0.123749	−0.123748	−0.122752	−0.0488922
	3	−0.0551947	−0.0551937	−0.054201	−0.00307324
	1	−0.498529	−0.498528	−0.497529	−0.405607
10	2	−0.12482	−0.124819	−0.123823	−0.0497771
	3	−0.0555123	−0.0555113	−0.0545186	−0.00318862
	1	−0.499805	−0.499804	−0.498806	−0.406866
20	2	−0.124979	−0.124978	−0.123982	−0.049909
	3	−0.0555589	−0.0555579	−0.0545652	−0.00320576
	1	−0.499943	−0.499942	−0.498943	−0.407001
30	2	−0.124996	−0.124995	−0.123999	−0.0499229
	3	−0.0555638	−0.0555628	−0.0545701	−0.00320755
	1	−0.5			
Exact	2	−0.125			
	3	−0.0555556			

The obtained eigenvalues are good, see Table V. The errors of the eigenvalues are about 0.3% for the first several states and increase with n. These errors cannot be reduced by decreasing ϵ, increasing Λ, or deceasing the step size h. The errors arise from the principal-value singularity left after subtraction.

C. Screened Cornell potential

In the case of the screened Cornell potential, the logarithmic singularity is removed by the Landé subtraction method while the double-pole singularity is relieved to be a principal-value singularity. As discussed in the preceding subsections, there will be no furcation phenomenon and the deviation is weakened in the obtained eigenfunctions when the extended Simpson's rule is applied to solve the truncated Eq. (39) as the screening parameters β and η are small. When β and η are large, the integrands can be well approximated by the extended Simpson's rule, and therefore the two peculiar phenomena disappear.

The obtained eigenvalues for the screened Cornell potential are listed in Table VI. The momentum-space results are compared with the coordinate-space results, and they agree well. Clearly, the results in momentum-space obtained by the Nyström method with the extended Simpson's rule are very accurate, especially when the screening parameters β and η are large.

D. Discussions

The furcation phenomenon can be used as an indicator for the bad behavior of the bad solutions and implies the bad behavior of the integrands. As discussed in the above subsections, the furcation effects appear in the solutions of different equations, such as the Schrödinger equation and the spinless Salpeter equation [39] with different potentials, such as the screened Coulomb potential, the screened

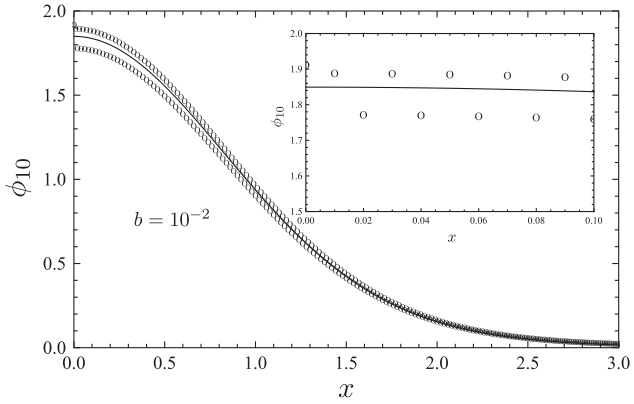

FIG. 3. The comparison between the ground state eigenfunctions for the subtracted equation (the solid line) (39) and for the original equation (the circles) (37) with the screened linear potential. The extended Simpson's rule is applied to solve numerically the eigenvalue equations. $x = p(\mu\lambda)^{-1/3}$, $b = \eta(\mu\lambda)^{-1/3}$, $\alpha = 0$.

linear potential, and the screened Cornell potential. Therefore, we expect the furcation phenomenon is system-independent.

The emergence of the furcation phenomenon indicates that the potential is singular and the numerical results are bad to some extent. That the furcation phenomenon does not occur does not mean the potential is free of singularity, for example, the furcation disappears in the eigenfunctions for the subtracted screened linear potential which has a principal-value singularity. As a result, the furcation phenomenon is only an indicator suggesting that the potential is singular and it does not represent singular potentials.

As discussed in the previous subsections, the deviation of the first point varies with the screening parameters β, η and the step h. If β, η are large enough, the integrals behave well and can be well approximated by the Simpson's rule and then the deviation disappears, see Figs. 1 and 2. The numerical results show that the deviation becomes weaker when the step h is smaller. Based on the numerical results obtained, we find the first point problem does not relate to the truncation, that is to say, the deviation does not vary with the upper limit Λ. Being a contrast to the weakened deviation for the screened Coulomb potential problem, it is interesting that the deviation disappears in the eigenfunctions for the subtracted equation with the screened linear potential. The method of completely solving the first point problem remains unknown to us, and further analysis is indeed planned.

TABLE V. The ratios $E_n/(\lambda^{2/3}\mu^{-1/3})$ for the screened linear potential with $l = 0$. $b = \eta(\mu\lambda)^{-1/3}$, $x = p(\mu\lambda)^{-1/3}$, $\alpha = 0$. $x_1 = 10^{-6}$, $h = 0.01$. The extended Simpson's rule is applied to solve the subtracted Eq. (39). The exact results with $b = 0$ are 1.85576, 3.24461 and 4.38167 for $n = 1$, $n = 2$ and $n = 3$, respectively.

x_N	n	$b = 10^{-6}$	$b = 10^{-3}$	$b = 10^{-1}$
	1	1.85235	1.85226	1.76429
5	2	3.23451	3.23423	2.96638
	3	4.36338	4.36288	3.87607
	1	1.85246	1.85237	1.7644
10	2	3.2346	3.23433	2.96649
	3	4.36345	4.36294	3.87618
	1	1.85249	1.8524	1.76443
20	2	3.23464	3.23436	2.96653
	3	4.36348	4.36298	3.87621
	1	1.8525	1.85241	1.76444
30	2	3.23464	3.23437	2.96653
	3	4.36349	4.36298	3.87622

TABLE VI. Energy eigenvalues (in GeV) for the screened Cornell potential with $l = 0$ are calculated in momentum space (MS) and in coordinate space (CS) respectively. $\mu = 0.625$GeV, $C = 0$ GeV, $\alpha = 0.3$, $\beta = 0$ GeV, $\lambda = 0.18$ GeV^2. $p_1 = 10^{-6}$ GeV, $h = 0.01$ GeV, $p_N = 20$ GeV. η is in GeV.

	Numerical (MS)		Numerical (CS)	
n	$\eta = 10^{-3}$	$\eta = 10^{-1}$	$\eta = 10^{-3}$	$\eta = 10^{-1}$
1	0.52622	0.47236	0.52774	0.47236
2	1.0929	0.90813	1.0982	0.90813
3	1.5322	1.1852	1.5421	1.1852
4	1.9121	1.3823	1.9274	1.3823
5	2.2549	1.5265	2.2762	1.5273

V. CONCLUSIONS

In this paper, we solve numerically the Schrödinger equations in momentum space with the screened Coulomb potential, the screened linear potential, and the screened Cornell potential, respectively, by employing the Nyström method with the extended Simpson's rule. Because of the bad behavior of the integrands arising from the singularities when the screening parameters η and β are small and the chosen quadrature rule with repeated unequal weights, the furcation phenomenon and deviation phenomenon emerge in the obtained eigenfunctions. The seeming drawback of the method is its merit in fact. We propose to use the furcation effect as an indicator for the bad behavior of the integrals and for the unreliability of the obtained numerical results.

We have shown that by using relatively simple mathematical structure, the Nyström method with the extended Simpson's rule, good precision in eigenvalues and eigenvectors can be obtained. Using the Landé subtraction method, the logarithmic singularity is removed and the singularity of the second order is weakened to be a principal-value singularity. In consequence, the furcation phenomenon vanishes, the deviation of the first point disappears or is weakened in the obtained eigenfunctions, the eigenvalues are obtained with very high accuracy, and the accuracy can be improved by adjusting the input parameters.

[1] E. Eichten, K. Gottfried, T. Kinoshita, J. B. Kogut, K. D. Lane, and T. M. Yan, Phys. Rev. Lett. **34**, 369 (1975); **36**, 1276(E) (1976).

[2] E. Eichten, K. Gottfried, T. Kinoshita, K. D. Lane, and T. M. Yan, Phys. Rev. D **17**, 3090 (1978); **21**, 313(E) (1980).

[3] E. Eichten, K. Gottfried, T. Kinoshita, K. D. Lane, and T. M. Yan, Phys. Rev. D **21**, 203 (1980).

[4] S. Godfrey and N. Isgur, Phys. Rev. D **32**, 189 (1985).

[5] G. S. Bali, Phys. Rep. **343**, 1 (2001).

[6] S. Uehara *et al.* (Belle Collaboration), Phys. Rev. Lett. **96**, 082003 (2006).

[7] P. Gonzalez, A. Valcarce, H. Garcilazo, and J. Vijande, Phys. Rev. D **68**, 034007 (2003).

[8] J. Vijande, P. Gonzalez, H. Garcilazo, and A. Valcarce, Phys. Rev. D **69**, 074019 (2004).

[9] J. Segovia, A. M. Yasser, D. R. Entem, and F. Fernandez, Phys. Rev. D **78**, 114033 (2008).

[10] J. Vijande, G. Krein, and A. Valcarce, Eur. Phys. J. A **40**, 89 (2009).

[11] J. Segovia, D. R. Entem, and F. Fernandez, Phys. Lett. B **662**, 33 (2008).

[12] E. H. Mezoir and P. Gonzalez, Phys. Rev. Lett. **101**, 232001 (2008).

[13] F. J. Rogers, H. C. Graboske, and D. J. Harwood, Phys. Rev. A **1**, 1577 (1970).

[14] J. McEnnan, L. Kissel, and R. H. Pratt, Phys. Rev. A **13**, 532 (1976).

[15] C. C. Gerry, J. Phys. A **17**, L313 (1984).

[16] H. Kröger, R. J. Slobodrian, and G. L. Payne, Phys. Rev. C **37**, 486 (1988).

[17] R. Girard, H. Kröger, P. Labelle, and Z. Bajzer, Phys. Rev. A **37**, 3195 (1988).

[18] S. Garavelli and F. A. Oliveira, Phys. Rev. Lett. **66**, 1310 (1991).

[19] O. A. Gomes, H. Chacham, and J. R. Mohallem, Phys. Rev. A **50**, 228 (1994).

[20] V. I. Yukalov, E. P. Yukalova, and F. A. Oliveira, J. Phys. A **31**, 4337 (1998).

[21] F. Brau, J. Phys. A **36**, 9907 (2003).

[22] W. H. Press, S. A. Teukolsky, W. T. Vetterling, and B. P. Flannery, Numerical Recipes in C: The Art of Scientific Computing (Cambridge University Press, New York, 1992).

[23] R. S. Anderssen, F. R. de Hoog, and M. A. Lukas, *The Application and Numerical Solution of Integral Equations* (Sijthoff and Noordhoff, Netherlands, 1980).

[24] K. E. Atkinson, *The Numerical Solution of Integral Equations of the Second Kind* (Cambridge University Press, New York, 1997).

[25] C. T. H. Baker, *The Numerical Treatment of Integral Equations* (Oxford University Press, New York, 1977).

[26] L. M. Delves and J. L. Mohamed, *Computational methods for integral equations* (Cambridge University Press, New York, 1992).

[27] A. Deloff, Ann. Phys. (N.Y.) **322**, 2315 (2007).

[28] G. Hardekopf and J. Sucher, Phys. Rev. A **30**, 703 (1984).

[29] R. H. Landau, Phys. Rev. C **27**, 2191 (1983).

[30] R. H. Landau, Phys. Rev. C **28**, 1324 (1983).

[31] A. Lande, as quoted in Ref. [29] above.

[32] Y. R. Kwon and F. Tabakin, Phys. Rev. C **18**, 932 (1978).

[33] R. H. Landau, *Quantum Mechanics II: A Second Course in Quantum Theory* (Wiley, New York, 1990).

[34] J. W. Norbury, D. E. Kahana, and K. M. Maung, Can. J. Phys. **70**, 86 (1992).

[35] K. M. Maung, D. E. Kahana, and J. W. Norbury, Phys. Rev. D **47**, 1182 (1993).

[36] J. W. Norbury, K. M. Maung, and D. E. Kahana, Phys. Rev. A **50**, 2075 (1994).

[37] A. Tang, arXiv:hep-ph/0103035.

[38] Strictly speaking, there will be no singularities in the screened Cornell potential if the screening parameters are greater than zero; however, the potential behaves badly when the screening parameters become small, and cannot be well approximated by the extended Simpson's rule. Therefore, we regard $p = p'$ as a singular point in this paper.

[39] J.-K. Chen (work in progress).

[40] C. Lubich, Numer. Math. **52**, 413 (1988).

[41] R. Courant and D. Hilbert, *Methods of Mathematical Physics I* (Interscience, New York, 1966).